J IRAN CHEM SOC (2014) 11:297–313
DOI 10.1007/s13738-013-0301-x

ORIGINAL PAPER

Potential bioactive Vanillin–Schiff base di- and tri-organotin(IV) complexes of 4-((3,5-dimethylphenylimino)methyl)-2-methoxyphenol: synthesis, characterization and biological screenings

Muhammad Sirajuddin · Saqib Ali · Farooq Ali Shah · Muhammad Ahmad · Muhammad Nawaz Tahir

Received: 29 April 2013 / Accepted: 20 June 2013 / Published online: 10 July 2013

Abstract Eight different di- and triorganotin(IV) complexes of vanillin-Schiff base of the type R_2SnClL and R_3SnL [R = Me (**1**,**6**), *n*-Bu (**2**,**7**), Ph (**3**,**8**), *tert*-Bu (**4**), Cy (**5**) and L = 4-((3,5-dimethylphenylimino)methyl)-2-methoxyphenol] were synthesized. The products were characterized by elemental analysis, FT-IR, ^{1}H, ^{13}C and ^{119}Sn NMR spectroscopy. The ligand 4-((3,5-dimethylphenylimino)methyl)-2-methoxyphenol is also characterized by single crystal X-ray analysis. In the ^{1}H NMR spectra of **1** and **6**, the $^{2}J(^{119/117}Sn\text{-}^{1}H)$ in the Sn-CH_3 moiety has 57 and 54 Hz values, respectively, that confirm the formation of four-coordinated Sn species. Moreover, the ^{13}C NMR value for *ipso* carbon of SnPh is 139 ppm which also confirms the formation of four-coordinated Sn species. The title ligand and its complexes were also screened for their biological activities such as interaction with DNA, enzymatic, antimicrobial, cytotoxic and antioxidant activities. The antimicrobial and cytotoxic activities of triorganotin(IV) derivatives are relatively higher than their corresponding diorganotin(IV) analogues due to their greater lipophilicity and permeability through cell membrane.

Electronic supplementary material The online version of this article (doi:10.1007/s13738-013-0301-x) contains supplementary material, which is available to authorized users.

M. Sirajuddin · S. Ali (✉) · F. A. Shah · M. Ahmad
Department of Chemistry, Quaid-i-Azam University, Islamabad 45320, Pakistan
e-mail: drsa54@yahoo.com

M. Sirajuddin
e-mail: m.siraj09@yahoo.com

M. N. Tahir
Department of Physics, University of Sargodha, Sargodha, Pakistan

Keywords Schiff base · Organotin(IV) compound · Crystal structure · DNA-binding · Enzymatic activity

Introduction

Schiff bases are studied widely due to their interesting characteristics, including photochromic and thermochromic properties, proton transfer tautomeric equilibria, biological and pharmacological activities, as well as suitability for analytical applications. Due to synthetic flexibility and simple preparation procedure these compounds have gained a great deal of attention as suitable ligands for coordination and determination of various metal ions [1]. Schiff base ligands are considered as "privileged ligands" due to their ease of preparation and their use as fluorogenic agent, pesticides, herbicidal agents, blocking agents, as well as catalysis [2]. Some of Schiff base complexes are used as model molecules for biological oxygen carrier systems [3]. Tetradentate Schiff base ligands are well known to form stable complexes, where the coordination takes place through the N_2O_2 donor set [4–6].

Over the recent decades, studies on coordination of Schiff bases to organotin(IV) compounds have got enormous attention with respect to their potential applications in medicinal chemistry and biotechnology and their structural variety [7–9]. Schiff base ligands are potential anticancer, anti-bacterial and anti-viral agents and these activities tend to increase in metal Schiff base complexes [10]. Schiff bases react with organotin(IV) halides to form variety of structures [11–13].

The study of organotin(IV) complexes has gained growing interest in the past few decades due to their ability to interact with DNA, signifying their potential application

in cancer chemotherapy [14–17]. Several organotin(IV) Schiff base complexes have been explored for their structural diversity and biocidal activities [18–20]. Cagnoli et al. [21], found some organotin(IV) complexes to be even more active in vitro than the clinically used *cis*-platin. Usually, triorganotin(IV) compounds exhibit a higher biological activity than their di- and monoorganotin(IV) analogues, which has been related to their ability to bind to proteins [22, 23]. Organotin(IV) compounds have been receiving increasing attention in recent years due to their antitumor activity and it has been observed that several diorganotin adducts show potentials antineoplastic and antituberculosis activities. Also, dialkyltin(IV) compounds have selective effects on lymphocytes, which can be used in cancer chemotherapy or to control other pathological effects [24]. Against human tumor cell lines, triphenyltin derivatives are highly active, being characterized by very low LD_{50} values [25].

The binding of small molecules with the DNA is of great importance because of advantages of these molecules as potential drugs. The concept of intercalation into DNA was first formulated by Lerman [26] in 1961; it has become widely recognized that many compounds of pharmacological interest, including anticancer drugs and antibiotics correlate their biological and therapeutic activities with the ability of intercalative interaction with DNA [27]. This non-covalent binding has an important function in life phenomena at the molecular level, deciding the interaction specificity of drug with DNA.

The study of drug–DNA interaction is important for understanding the molecular mechanisms of the drug action and designing specific DNA-targeted drugs [28]. Such interactions are studied using a variety of techniques like cyclic voltammetry, UV–visible, fluorescence, Raman and NMR spectroscopy [29]. The interaction of some metal chelates of Co(III), Ru(II) and Os(II) with DNA were studied by cyclic voltammetry [30], but their lower affinity to DNA encouraged the researchers to concentrate their effort on other potential metal complexes. Interest about DNA–organotin(IV) systems arises from the large industrial uses of organotins, their consequent spread out in the environment and the related biological actions [31, 32].

In the present study we have synthesized a Schiff base ligand and its complexes with tri- and diorganotin(IV) compounds. The synthesized ligand and its complexes were characterized by various techniques including FT-IR, NMR, elemental analysis and single crystal analysis. Biological aspects including interaction with DNA, enzyme inhibition, antibacterial, antifungal, cytotoxic and antioxidant activities of the synthesized ligand and its complexes were studied.

Experimental

Materials and methods

Reagents, Me_3SnCl, *n*-Bu_3SnCl, *tert*-Bu_3SnCl, Ph_3SnCl, Cy_3SnCl, vanillin, 3,5-dimethylaniline were obtained from Aldrich (USA) and were used without further purification. All the solvents purchased from E. Merck (Germany) were dried before use according to the literature procedure [33]. The melting points were determined in a capillary tube using a Gallenkamp (UK) electrothermal melting point apparatus. IR spectra in the range of 4,000–100 cm^{-1} were obtained on a Thermo Nicolet-6700 FT-IR Spectrophotometer. Microanalysis was done using a Leco CHNS 932 apparatus. ^{1}H and ^{13}C NMR were recorded on a Bruker-300 MHz FT-NMR Spectrometer, using $CDCl_3$ as an internal Ref. [^{1}H ($CDCl_3$) = 7.25 and ^{13}C ($CDCl_3$) = 77]. Chemical shifts are given in ppm and coupling constants (J) values are given in Hz. The multiplicities of signals in ^{1}H NMR are given with chemical shifts; (s = singlet, d = doublet, t = triplet, m = multiplet). ^{119}Sn-NMR spectra were recorded at 298 K of samples dissolved in DMSO-d6 with a 400 MHz JEOL ECS instrument. The measurements were recorded at a working frequency of 149.4 MHz and the chemical shifts were referenced to Me_4Sn as external standard. The absorption spectra were measured on a Shimadzu 1800 UV–Visible Spectrophotometer. Viscosity was measured by Ubbelohde viscometer at room temperature. The electrical conductance was measured on a WTW Series Inolab Cond 720. The GC-MS spectrum was taken on a gas chromatograph, model GC-6890 N coupled with mass Spectrometer, model MS-5973 MSD (mass selective detector). Separation was performed on a capillary column DB-5MS (30 m × 0.32 mm, 0.25 μm of film thickness). The mass Spectrometer coupled with GC was set to scan in the range of m/z 50–550 with electron impact (EI) mode of ionization. The X-ray diffraction data were collected on a Bruker SMART APEX CCD diffractometer, equipped with a 4 K CCD detector set 60.0 mm from the crystal. The crystals were cooled to 100 ± 1 K using the Bruker KRYOFLEX low-temperature device and Intensity measurements were performed using graphite monochromated Mo-Kα radiation from a sealed ceramic diffraction tube (SIEMENS). Generator settings were 50 kV/40 mA. The structure was solved by Patterson methods and extension of the model was accomplished by direct methods using the program DIRDIF or SIR2004. Final refinement on F_2 carried out by full-matrix least squares techniques using SHELXL-97, a modified version of the program PLUTO (preparation of illustrations) and PLATON package.

Synthesis

Synthesis of ligand: 4-((3,5-dimethylphenylimino)methyl)-2-methoxyphenol (HL)

Stoichiometric amounts of vanillin and 3,5-dimethylaniline (5 mmol of each) were added to freshly dried toluene. The reaction mixture was stirred and refluxed for 3–4 h and the water formed during the reaction was removed using Dean and Stark apparatus. Volume of the reaction mixture was reduced to one-third of its original solvent volume and left to crystallize at room temperature. The red crystals of **HL** suitable for single crystal analysis were isolated from the mother liquor and dried. The chemical reaction is shown in Scheme 1.

Yield: 85 %, m.p.: 99 °C, Anal. Calc. for $C_{16}H_{17}NO_2$: mol. wt.: 255.31, C, 75.27; H, 6.71; N, 5.49, Found: C, 75.30; H, 6.70; N, 5.50 %, IR (cm^{-1}): *v* 1,625 (C=N), 1,426 and 1,581 (Ar C=C), 3,320 (OH), 1,252 (Phen. C–O str. vib.), ^{1}H NMR ($CDCl_3$, ppm): 2.38 (s, 6H, H1, H1′), 6.90 (s, 1H, H3), 6.87 (s, 2H, H4, H4′), 8.37 (s, 1H, H6), 7.24 (s, 1H, H8), 7.64 (d, 1H, H9, $^3J[^1H\text{-}^1H] = 9$ Hz), 6.99 (d, 1H, H10, $^3J[^1H\text{-}^1H] = 9$ Hz), 6.61 (s, 1H, OH), 3.94 (s, 3H, H13), ^{13}C NMR ($CDCl_3$, ppm): 21.4 (2C, C1, C1′), 138.8 (2C, C2, C2′), 129.1 (1C, C3), 118.7 (2C, C4, C4′), 149.1 (1C, C5), 160 (1C, C6), 127.4 (1C, C7), 108.5 (1C, C8), 125.3 (1C, C9), 114.3 (1C, C10), 147 (1C, C11), 152.1 (1C, C12), 56.0 (1C, C13), molar conductance (Λ_m, $S.cm^2.mol^{-1}$): 13 at 25 °C.

*General procedure for the synthesis of organotin(IV) Schiff base complexes (**1**–**8**)*

1.28 g (5 mmol) of **HL** was dissolved in 60 mL freshly dried toluene and to it 0.69 mL (5 mmol) of Et_3N was added. The reaction mixture was stirred and refluxed for about 30 min and then calculated amount (5 mmol) of R_3SnCl and R_2SnCl_2 (R = Me (**1**), *n*-Bu (**2**), Ph (**3**), *tert*-Bu (**4**), Cy (**5**)) was added (Scheme 2). The reaction mixture was again stirred and refluxed for about 6–7 h. The mixture was then allowed to stand overnight so that triethylammoniun chloride salt may settle down. The contents of the flask were then filtered till no further formation of triethylammoniun chloride salt occurred and the filtrate was rotary evaporated to get the desire product.

*Trimethyltin(IV) 4-((3,5-dimethylphenylimino)methyl)-2-methoxyphenolate; (**1**)*

Yield: 78 %, molecular formula: $C_{19}H_{25}NO_2Sn$, mol. wt.: 418.12, physical state: liquid, IR (cm^{-1}): *v* 1,625 (C=N), 1,427 and 1,581 (Ar. C=C), 1,280 (Phen. C-O str. vib.), 546 (Sn-C), 464 (Sn-O), ^{1}H NMR ($CDCl_3$, ppm): 2.41 (s, 6H, H1, H1′), 6.95 (s, 1H, H3), 6.92 (s, 2H, H4, H4′), 8.4 (s, 1H, H6), 7.25 (s, 1H, H8), 7.67 (d, 1H, H9, $^3J[^1H\text{-}^1H] = 9$ Hz)), 7.00 (d, 1H, H10, $^3J[^1H\text{-}^1H] = 9$ Hz), 3.92 (s, 3H, H13), 0.64 (s, Sn-CH_3, $^2J[^{119/117}Sn\text{-}^1H = 57, 56$ Hz]), ^{13}C NMR ($CDCl_3$, ppm): 21.9 (2C, C1, C1′), 138.8 (2C, C2, C2′), 129.1 (1C, C3), 118.8 (2C, C4, C4′), 149.2 (1C, C5), 160.1 (1C, C6), 127.4 (1C, C7), 108.6 (1C, C8), 125.4 (1C, C9), 113.3 (1C, C10), 148.0 (1C, C11), 153.3 (1C, C12) 55.7 (1C, C13), 20.9 (Sn-CH_3, $^1J[^{119/117}Sn\text{-}^1H = 389, 372$ Hz])), ^{119}Sn NMR (DMSO, ppm): −200.5, molar conductance (Λ_m, $S.cm^2.mol^{-1}$): 15 at 25 °C.

Tri-n-butyltin(IV) 4-((3,5-dimethylphenylimino)methyl)-2-methoxyphenolate; (2)

Yield: 75 %, molecular formula: $C_{28}H_{43}NO_2Sn$, mol. wt.: 544.36, physical state: liquid, IR (cm^{-1}): *v* 1,625 (C=N), 1,427 and 1,582 (Ar. C=C), 1,282 (Phen. C-O str. vib.), 558 (Sn-C), 464 (Sn-O), ^{1}H NMR ($CDCl_3$, ppm): 2.39 (s, 6H, H1, H1′), 6.99 (s, 1H, H3), 6.89 (s, 2H, H4, H4′), 8.37 (s, 1H, H6), 7.25 (s, 1H, H8), 7.67 (d, 1H, H9, $^3J[^1H\text{-}^1H] = 9$ Hz), 6.99 (d, 1H, H10, $^3J[^1H\text{-}^1H] = 9$ Hz), 3.91 (s, 3H, H13), 1.30 (t, 2H, Hα, $^3J[^1H\text{-}^1H] = 16.5$ Hz), 1.65 (m, 2H, Hβ), 1.31 (m, 2H, Hγ, 0.95 (t, 3H, Hδ, $^3J[^1H\text{-}^1H] = 14.7$ Hz), ^{13}C NMR ($CDCl_3$, ppm): 21.4 (2C, C1, C1′), 138.7 (2C, C2, C2′), 129.1 (1C, C3), 118.8 (2C, C4, C4′), 149.4 (1C, C5), 160.1 (1C, C6), 127.3 (1C, C7), 108.6 (1C, C8), 125.4 (1C, C9), 113.2 (1C, C10), 147.4 (1C, C11), 153.2 (1C, C12), 55.8 (1C, C13), 19.7 (Cα, $^1J[^{119/117}$ Sn-^{13}Cα] = 395, 383 Hz), 27 (Cβ, $^2J[^{119}$Sn-^{13}Cβ] = 22 Hz), 28 (Cγ, $^3J[^{119}$Sn-^{13}Cγ] = 63 Hz), 14 (Cδ) ($SnCH_2CH_2CH_2CH_3$), ^{119}Sn NMR (DMSO, ppm):

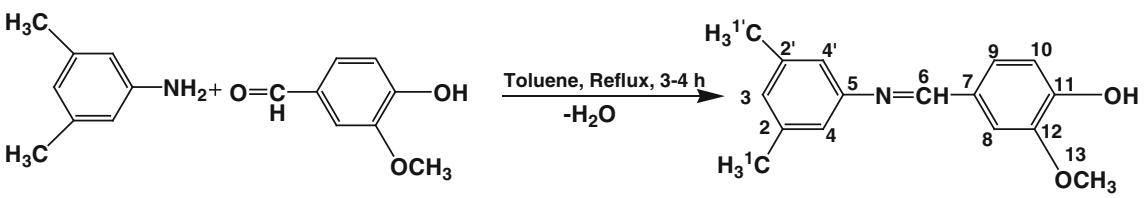

Scheme 1 Chemical reaction and structural representation of ligand (HL)

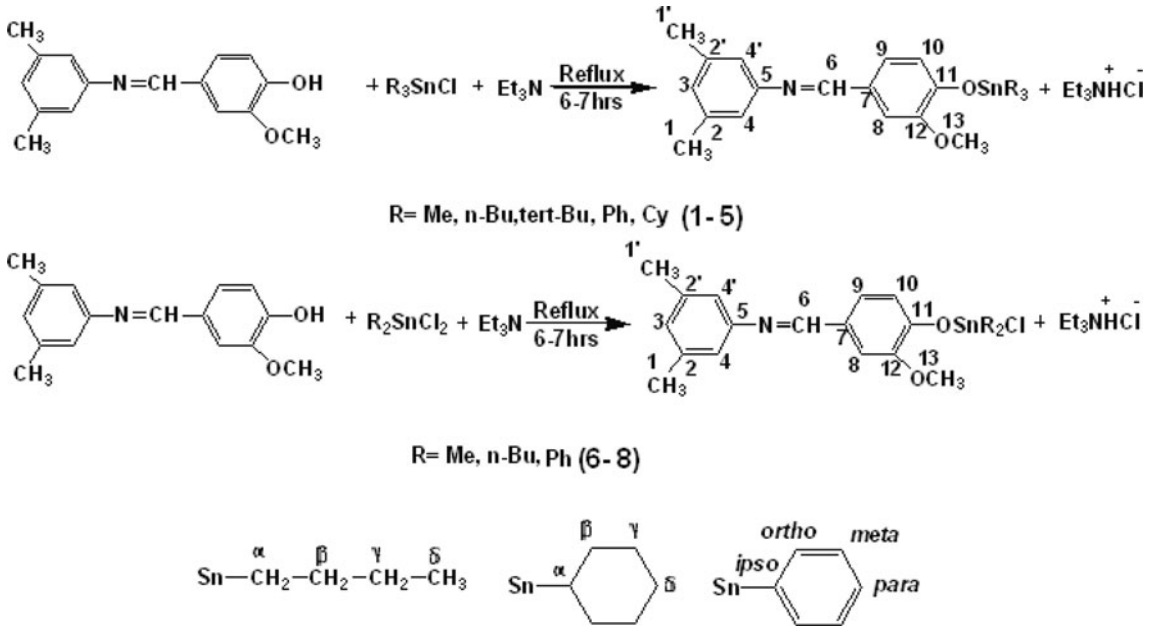

Scheme 2 Chemical reaction and structural representation of organotin(IV) Schiff base complexes along with numbering

−198.4: molar conductance (Λ_m, S.cm^2.mol^{-1}): 19 at 25 °C.

Triphenyltin(IV) 4-((3,5-dimethylphenylimino)methyl)-2-methoxyphenolate; (3)

Yield: 78 %, molecular formula: $C_{34}H_{31}NO_2Sn$, mol. wt.: 604.33, physical state: liquid, IR (cm^{-1}): *ν* 1,625 (C=N), 1,428 and 1,582 (Ar. C=C), 1,280 (Phen. C-O str. vib.), 555 (Sn-C), 451 (Sn-O), ^{1}H NMR ($CDCl_3$, ppm): 2.41 (s, 6H, H1, H1′), 6.93 (s, 1H, H3), 6.91 (s, 2H, H4, H4′), 8.40 (s, 1H, H6), 7.25 (s, 1H, H8) 7.64 (d, 1H, H9, $^3J[^1H\text{-}^1H] = 9$ Hz), 7.06 (d, 1H, H10), $^3J[^1H\text{-}^1H] = 9$ Hz), 3.92 (s, 3H, H13), 7.72–7.77 (m, 1H, Hβ), 7.48–7.55 (m, 1H, Hγ), 7.27–7.33 (m, 1H, Hδ), ^{13}C NMR ($CDCl_3$, ppm): 21.4 (2C, C1, C1′), 138.8 (2C, C2, C2′), 129.1 (1C, C3), 118.8 (2C, C4, C4′), 149.1 (1C, C5), 160 (1C, C6), 127.3 (1C, C7), 108.6 (1C, C8), 125.4 (1C, C9), 113.2 (1C, C10), 147.4 (1C, C11), 153.1 (1C, C12), 55.6 (1C, C13), 139 (C_{ipso}), 136.2 (C_{ortho}), 129.1 (C_{meta}), 129.9 (C_{para}) (SnPh),) $^2J[^{119/117}Sn\text{-}^{13}C_{ortho}] = 49$ Hz, $^3J[^{119}Sn\text{-}^{13}C_{meta}] = 63$ Hz, ^{119}Sn NMR (DMSO, ppm): −205: molar conductance (Λ_m, S.cm^2.mol^{-1}): 18 at 25 °C.

*Tri-tert-butyltin(IV) 4-((3,5-dimethylphenylimino)methyl)-2-methoxyphenolate; (**4**)*

Yield: 75 %, molecular formula: $C_{28}H_{43}NO_2Sn$, mol. wt.: 544.36, m.p: 89–91 °C, Anal. Calc. for $C_{28}H_{43}NO_2Sn$: C, 61.78; H, 7.96; N, 2.57; found: C, 61.75; H, 7.95; N, 2.59 %, IR (cm^{-1}): *ν* 1,625 (C=N), 1,426 and 1,581 (Ar. C=C), 1,280 (Phen. C-O str. vib.), 557 (Sn-C), 464 (Sn-O), ^{1}H NMR ($CDCl_3$, ppm): 2.37 (s, 6H, H1, H1′), 6.89 (s, 1H, H3), 6.86 (s, 2H, H4, H4′), 8.36 (s, 1H, H6), 7.24 (s, 1H, H8) 7.42 (d, 1H, H9, $^3J[^1H\text{-}^1H] = 9$ Hz), 6.99 (d, 1H, H10, $^3J[^1H\text{-}^1H] = 9$ Hz), 3.96 (s, 3H, H13), 1.28 (s, 27H, {Sn–C(CH$_3$)$_3$}, $^3J[^{119/117}Sn\text{-}^1H] = 117$, 112.2 Hz): ^{13}C NMR ($CDCl_3$, ppm): 21.4 (2C, C1, C1′), 138.8 (2C, C2, C2′), 129.1 (1C, C3), 118.7 (2C, C4, C4′), 149.1 (1C, C5), 159.9 (1C, C6), 127.4 (1C, C7), 108.5 (1C, C8), 125.3 (1C, C9), 113.2 (1C, C10), 147.3 (1C, C11), 153.2 (1C, C12), 56.0 (1C, C13), 44.5 (Cα, $^1J[^{119/117}Sn\text{-}^{13}C] = 468$, 447 Hz), 30 (Cβ, $^2J[^{119}Sn\text{-}^{13}C] = 138$ Hz): ^{119}Sn NMR (DMSO, ppm): −190.3: molar conductance (Λ_m, S.cm^2.mol^{-1}): 15 at 25 °C.

Tricyclohexyltin(IV) 4-((3,5-dimethylphenylimino)methyl)-2-methoxyphenolate; (5)

Yield: 73 %, molecular formula: $C_{34}H_{49}NO_2Sn$, mol. wt.: 622.47, m.p: 93–95 °C, Anal. Calc. for $C_{34}H_{49}NO_2Sn$: C, 65.60; H, 7.93; N, 2.25; found: C, 65.50; H, 7.89; N, 2.28 %, IR (cm^{-1}): *ν* 1,624 (C=N), 1,427 and 1,582 (Ar. C=C), 1,279 (Phen. C-O str. vib.), 560 (Sn-C), 491 (Sn-O), ^{1}H NMR ($CDCl_3$, ppm): 2.37 (s, 6H, H1, H1′), 6.89 (s, 1H, H3), 6.85 (s, 2H, H4, H4′), 8.36 (s, 1H, H6), 7.24 (s, 1H, H8) 7.62 (d, 1H, H9, $^3J[^1H\text{-}^1H] = 9$ Hz), 6.98 (d, 1H, H10, $^3J[^1H\text{-}^1H] = 9$ Hz), 3.98 (s, 3H, H13), 1.30 (m, 1H, Hα), 1.63 (m, 2H, Hβ), 1.84 (m, 2H, Hγ), 1.84 (m, 2H, Hδ), ^{13}C NMR ($CDCl_3$, ppm): 21.3 (2C, C1, C1′), 138.8 (2C, C2,

C2′), 129.2 (1C, C3), 118.7 (2C, C4, C4′), 149.0 (1C, C5), 160 (1C, C6), 127.3 (1C, C7), 108.4 (1C, C8), 125.2 (1C, C9), 114.2 (1C, C10), 147.1 (1C, C11), 153.5 (1C, C12), 56.1 (1C, C13), 33.8 (Cα, $^{1}J[^{119/117}Sn\text{-}^{13}C\alpha] = 316$, 302 Hz), 29 (Cβ, $^{2}J[^{119/117}Sn\text{-}^{13}C\beta] = 65$, 62 Hz), 31 (Cγ, $^{3}J[^{119/117}Sn\text{-}^{13}C\gamma] = 15$ Hz), 27 (Cδ, $^{4}J[^{119}Sn\text{-}^{13}C\delta] = 8$ Hz), ^{119}Sn NMR (DMSO, ppm): −226.1: molar conductance (Λ_m, S.cm^2.mol^{-1}): 16 at 25 °C.

*Dimethyltin(IV) [4-((3,5-dimethylphenylimino)methyl)-2-methoxyphenolate]chloride; (**6**)*

Yield: 70 %, molecular formula: $C_{18}H_{22}ClNO_2Sn$, mol. wt.: 438.54, m.p: 150–152 °C, Anal. Calc. for $C_{18}H_{22}ClNO_2Sn$: C, 49.30; H, 5.06; N, 3.19; found: C, 49.33; H, 5.02; N, 3.20 %, IR (cm^{-1}): *ν* 1,625 (C=N), 1,427 and 1,586 (Ar. C=C), 1,279 (Phen. C-O Str. vib.), 555 (Sn-C), 490 (Sn-O), 302 (C-Cl), ^{1}H NMR ($CDCl_3$, ppm): 2.37 (s, 6H, H1, H1′), 6.89 (s, 1H, H3), 6.85 (s, 2H, H4, H4′), 8.35 (s, 1H, H6), 7.24 (s, 1H, H8), 7.63 (d, 1H, H9, $^{3}J[^{1}H\text{-}^{1}H] = 9$ Hz), 6.98 (d, 1H, H10, $^{3}J[^{1}H\text{-}^{1}H] = 9$ Hz), 3.92 (s, 3H, H13), 1.08 (s, Sn–CH_3), $^{2}J[^{119}Sn\text{-}^{1}H] = 54$ Hz), ^{13}C NMR ($CDCl_3$, ppm): 21.4 (2C, C1, C1′), 138.8 (2C, C2, C2′), 129.1 (1C, C3), 118.7 (2C, C4, C4′), 148.9 (1C, C5), 159.7 (1C, C6), 127.3 (1C, C7), 108.4 (1C, C8), 125.2 (1C, C9), 113.1 (1C, C10), 147.1 (1C, C11), 153.7 (1C, C12) 55 (1C, C13), 20.3 (Cα, $^{1}J[^{119}Sn\text{-}^{13}C] = 386$ Hz), ^{119}Sn NMR (DMSO, ppm): −190 Hz, molar conductance (Λ_m, S.cm^2.mol^{-1}): 14 at 25 °C.

Di-n-butyltin(IV) [4-((3,5-dimethylphenylimino)methyl)-2-methoxyphenolate]chloride; (7)

Yield: 81 %, molecular formula: $C_{24}H_{34}ClNO_2Sn$, mol. wt.: 522.7, m.p: 89–90 °C, Anal. Calc. for $C_{24}H_{34}ClNO_2Sn$: C, 55.15; H, 6.56; N, 2.68; found: C, 55.20; H, 6.60; N, 2.65 %, IR (cm^{-1}): *ν* 1,623 (C=N), 1,427 and 1,583 (Ar. C=C), 1,275 (Phen. C-O str. vib.), 555 (Sn-C), 464 (Sn-O), 303 (C-Cl), ^{1}H NMR ($CDCl_3$, ppm): 2.37 (s, 6H, H1, H1′), 6.9 (s, 1H, H3), 6.88 (s, 2H, H4, H4′), 8.36 (s, 1H, H6), 7.24 (s, 1H, H8), 7.66 (d, 1H, H9, $^{3}J[^{1}H\text{-}^{1}H] = 9$ Hz), 6.99 (d, 1H, H10, $^{3}J[^{1}H\text{-}^{1}H] = 9$ Hz), 3.94 (s, 3H, H13), 1.01 (t, 2H, Hα, $^{3}J[^{1}H\text{-}^{1}H] = 15.5$ Hz), 1.81 (m, 2H, Hβ), 1.40 (m, 2H, Hγ), 0.95 (t, 3H, Hδ,, $^{3}J[^{1}H\text{-}^{1}H] = 13.5$ Hz) : ^{13}C NMR ($CDCl_3$, ppm): 21.3 (2C, C1, C1′), 138.8 (2C, C2, C2′), 129.1 (1C, C3), 118.9 (2C, C4, C4′), 148.4 (1C, C5), 159.9 (1C, C6), 127.4 (1C, C7), 108.6 (1C, C8), 125.3 (1C, C9), 113.3 (1C, C10), 147.3 (1C, C11), 152 (1C, C12), 56 (1C, C13), 21 (Cα, $^{1}J[^{119/117}Sn\text{-}^{13}C\alpha] = 398$, 385 Hz), 27 (Cβ, $^{2}J[^{119}Sn\text{-}^{13}C\beta] = 49$ Hz), 27 (Cγ, $^{3}J[^{119}Sn\text{-}^{13}C\gamma] = 62$ Hz), 14 (Cδ) ($SnCH_2CH_2CH_2CH_3$), ^{119}Sn NMR (DMSO, ppm): −192.2: molar conductance (Λ_m, S.cm^2.mol^{-1}): 15 at 25 °C.

Diphenyltin(IV) [4-((3,5-dimethylphenylimino)methyl)-2-methoxyphenolate]chloride; (8)

Yield: 70 %, molecular formula: $C_{28}H_{26}ClNO_2Sn$, mol. wt.: 562.67, m.p: 110–112 °C: Anal. Calc. for $C_{28}H_{26}ClNO_2Sn$: C, 59.77; H, 4.66; N, 2.49; found: C, 59.20; H, 4.60; N, 2.55 %.: IR (cm^{-1}): *ν* 1,625 (C=N), 1,427 and 1,580 (Ar. C=C), 1,280 (Phen. C-O str. vib.), 558 (Sn-C), 451 (Sn-O), 303 (Sn-Cl), ^{1}H NMR ($CDCl_3$, ppm): 2.50 (s, 6H, H1, H1′), 6.93 (s, 1H, H3), 7.02 (s, 2H, H4, H4′), 8.47 (s, 1H, H6), 7.25 (s, 1H, H8) 7.55 (d, 1H, H9, $^{3}J[^{1}H\text{-}^{1}H] = 9$ Hz), 7.10 (d, 1H, H10), 3.94 (s, 3H, H13), 7.60 (m, 1H, Hβ), 7.48 (m, 1H, Hγ), 7.40 (m, 1H, Hδ), ^{13}C NMR ($CDCl_3$, ppm): 21.4 (2C, C1, C1′), 138.9 (2C, C2, C2′), 129.1 (1C, C3), 118.9 (2C, C4, C4′), 149.7 (1C, C5), 160.4 (1C, C6), 127.6 (1C, C7), 108.8 (1C, C8), 125.5 (1C, C9), 113.4 (1C, C10), 147.7 (1C, C11), 153.2 (1C, C12), 55.9 (1C, C13), 139 (C_{ipso}), 136.2 (C_{ortho}), 129.2 (C_{meta}), 129.9 (C_{para}) (SnPh), $^{2}J[^{119}Sn\text{-}^{13}C_{ortho} = 64$ Hz], $^{3}J[^{119}Sn\text{-}^{13}C_{meta} = 49$ Hz],) $^{4}J[^{119/117}Sn\text{-}^{13}C_{para} = 13$ Hz], ^{119}Sn NMR (DMSO, ppm): −200: molar conductance (Λ_m, S.cm^2.mol^{-1}): 17 at 25 °C.

Studies of DNA interaction by UV–visible spectroscopy

CT-DNA (20 mg) was dissolved in double-deionized water (pH = 7.0) and stored at 4 °C. The nucleotide to protein (N/P) ratio of ~1.9 was obtained from the ratio of absorbance at 260 and 280 nm ($A_{260}/A_{280} = 1.9$), indicating that the DNA is sufficiently free from protein [34]. The DNA concentration was determined via absorption spectroscopy using the molar absorption coefficient of 6,600 M^{-1}cm^{-1} (260 nm) for CT-DNA [35]. The compounds were dissolved in 80 % ethanol at a concentration of 0.392 mM. The UV absorption spectra were obtained by keeping the concentration of the compound fixed while varying the DNA concentration. Equivalent solutions of DNA were added to the complex and reference solutions to eliminate the absorbance of DNA itself. Compound-DNA solutions were allowed to incubate for 30 min at room temperature before measurements were made. Absorption spectra were recorded using cuvettes of 1 cm path length at room temperature.

Enzymatic activity

Assay of alkaline phosphatase activity

The inhibition of alkaline phosphatase was assayed by monitoring the rate of hydrolysis of *p*-nitrophenyl phosphate at 25 °C in 0.1 M Na_2CO_3-$NaHCO_3$ (sodium carbonate–bicarbonate) buffer (pH 10.1) [36, 37]. The enzyme

Scheme 3 Hydrolysis of *p*-nitrophenyl phosphate catalyzed by alkaline phosphatase

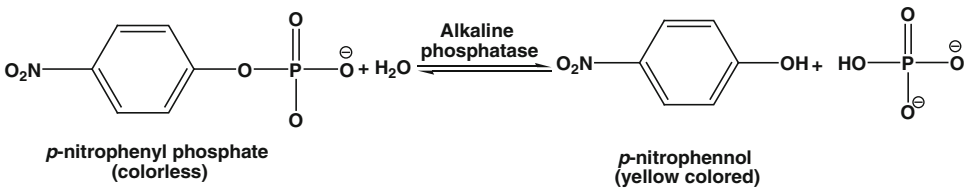

catalyzes the hydrolysis of phosphate monoesters resulting in the formation of inorganic phosphate and an alcohol. The identity of the alcohol varies depending on the specific phosphatase. The assay of alkaline phosphatase activity takes advantage of the fact that the enzyme is non-specific and utilizes the non-biological substrate *p*-nitrophenyl phosphate (colorless) to give yellow-colored *p*-nitrophenol upon hydrolysis which helps to monitor the reaction as shown in Scheme 3 [37].

Stock solutions of 50 μM inhibitors (compounds) in one mL DMSO were prepared at room temperature. The buffer and substrate were mixed in 1:4 ratio to make the reagent solution. Then from the reagent solution 2,000 μL (2 mL) was taken in the cell to which 40 μL enzyme and varying concentrations of the inhibitor were added. The activity of the alkaline phosphatase in the presence and absence of inhibitor was measured spectrophotometerically. The release of yellow-colored *p*-nitrophenol chromophore was monitored at 405 nm wavelength. Enzyme activity has been expressed as the μM of *p*-nitrophenol released per min for 5 min for each concentration of the inhibitor and then their average value taken. The inhibition of enzyme by inhibitor was calculated by the following formula [38]:

$$\text{Units/mL enzyme} = \frac{\left(\frac{\Delta A405\,\text{nm}}{\text{min Test}} - \frac{\Delta A405\,\text{nm}}{\text{min Blank}}\right) \text{total VmL(reagent + enzyme + inhibitor)} \times \text{D.F}}{18.5 \times \text{VmL of enzyme taken}} \quad (1)$$

D.F = Dilution factor.

18.5 = Millimolar extinction coefficient of *p*-nitrophenol at 405 nm.

By the addition of inhibitor the activity of the enzyme decreased and at higher concentration it was almost completely inhibited in some cases.

DPPH free radical scavenging activity

A methanol solution of the free radical DPPH$^{\cdot}$ of absorption approximately 0.9 was mixed with a proper amount of methanol solution of an antioxidant (compound). Free radical scavenging activity of the synthesized ligand **HL** and some of the representative organotin(IV) complexes (**1, 3, 5** and **7**) was determined by measuring the change in the absorbance of DPPH$^{\cdot}$ (1,1-diphenyl-2-picrylhydrazylradical) at 517 nm spectrophotometerically. Stock solutions of 500 μM of all tested samples and DPPH$^{\cdot}$ were prepared in methanol and 400 μL of DPPH$^{\cdot}$ solution was added to sample solutions at different concentrations (500, 1,000, 1,500, 2,000 and 2,500 μL) and appropriately diluted with methanol to total volume of 3.0 mL. 400 μL of DPPH$^{\cdot}$ stock solution was also diluted to 3.0 mL using methanol solvent to make the control. The mixture was then incubated for 40 min at room temperature and in darkness. During incubation, a reduction occurred of a part of the free radical form DPPH$^{\cdot}$, dependent on the concentration of the antioxidant added. Then, absorption was measured at a characteristic DPPH$^{\cdot}$ wavelength equal to 517 nm and absorption of the solvent was corrected throughout using the same solvent in the reference cell. The scavenging effect was calculated using the following equation [39, 40]:

$$\text{Scavenging activity}\,(\%) = \frac{A_o - A_s}{A_o} \times 100 \quad (2)$$

where A_s is the absorbance of the DPPH$^{\cdot}$ in the presence of the tested compound and A_o is the absorbance of the DPPH$^{\cdot}$ in the absence of the tested compound (control). The data for antioxidation are presented as mean ± SD of three determinations.

Antibacterial assay

The synthesized ligand and its organotin(IV) complexes were tested against six bacterial strains: two Gram-Positive [*Micrococcus luteus* (ATCC10240) and *Staphylococcus aureus* (ATCC6538)] and four Gram-negative [*Escherichia coli* (ATCC15224), *Enterobacter aerogenes* (ATCC13048), *Bordetella bronchiseptica* (ATCC4617) and *Klebsiella pneumonia* (MTCC618)]. The agar well-diffusion method was used for the determination of antibacterial activity [41]. Broth culture (0.75 mL) containing ca. 10^6 colony-forming units (CFU) per mL of the test strain was added to 75 mL of nutrient agar medium at 45 °C, mixed well, and then poured into a 14-cm sterile petri plate. The media was allowed to solidify, and 8 mm wells were dug with a sterile metallic borer. Then a DMSO solution of test sample (100 μL) at 1 mg/mL was added to the respective wells. DMSO served as negative control, and the standard antibacterial drugs *Roxyithromycin* (1 mg/mL) and *Cefixime* (1 mg/mL) were used as positive control. Triplicate plates of each bacterial strain were prepared which were incubated aerobically at 37 °C for 24 h. The

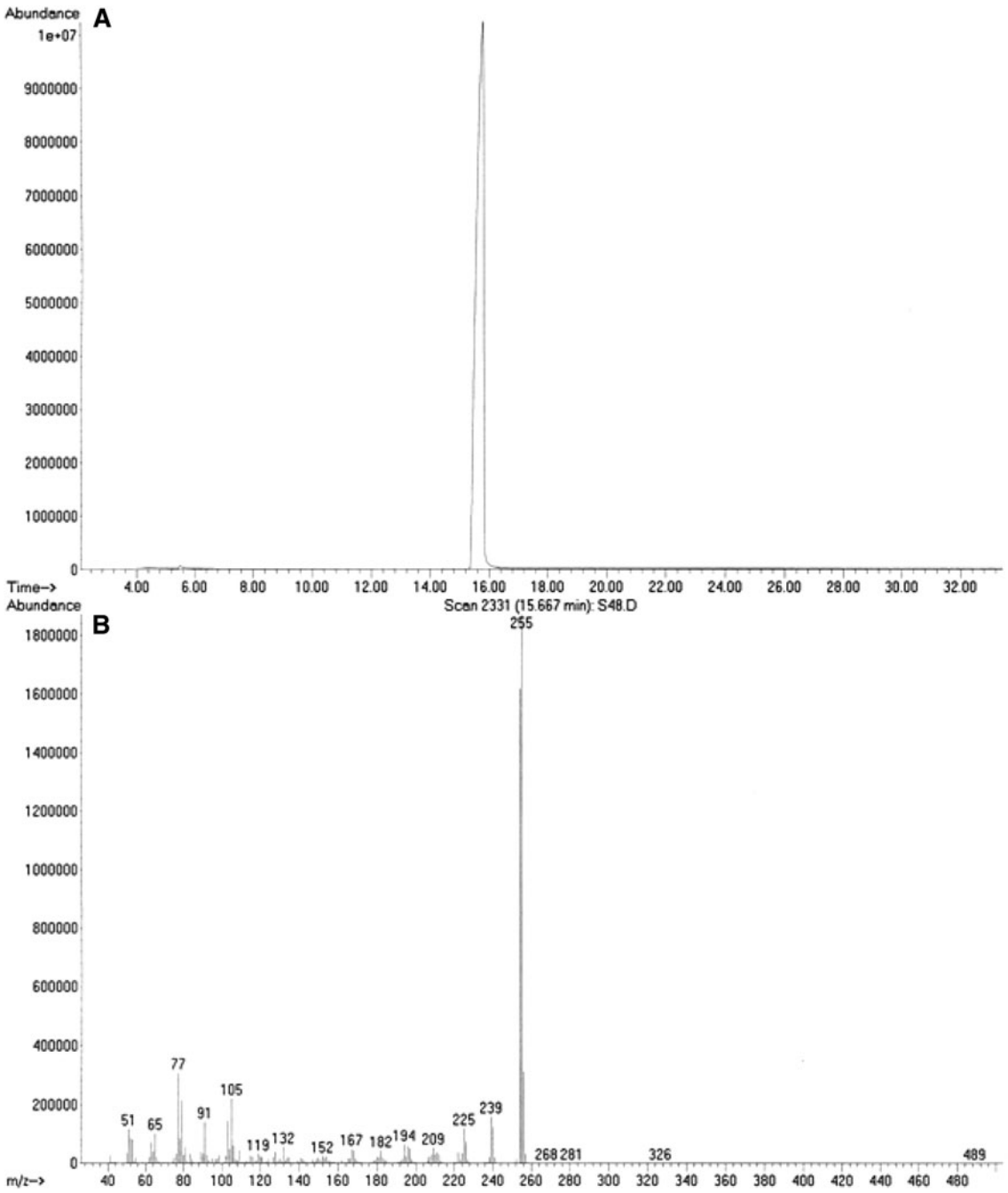

Fig. 1 GC-MS spectrum of HL. **a** GC spectrum and **b** MS spectrum

activity was determined by measuring the diameter of zone showing complete inhibition (mm).

Antifungal assay

Antifungal activity against five fungal strains (*Fusarium moniliformis*, *Aspergillus niger*, *Fusarium solani*, *Mucor species* and *Aspergillus fumigatus*) was determined using Agar tube dilution method [41]. Screw capped test tubes containing Sabouraud dextrose agar (SDA) medium (4 mL) were autoclaved at 121 °C for 15 min. Tubes were allowed to cool at 50 °C and non-solidified SDA was loaded with 66.6 µL of compound from the stock solution (12 mg/mL in DMSO) to make 200 µg/mL final concentration. Tubes were then allowed to solidify in slanting position at room temperature. Each tube was inoculated with 4 mm diameter piece of inoculum from 7-day-old fungal culture. The media supplemented with DMSO and *Turbinafine* (200 µg/mL) were used

Scheme 4 Fragmentation pattern of HL

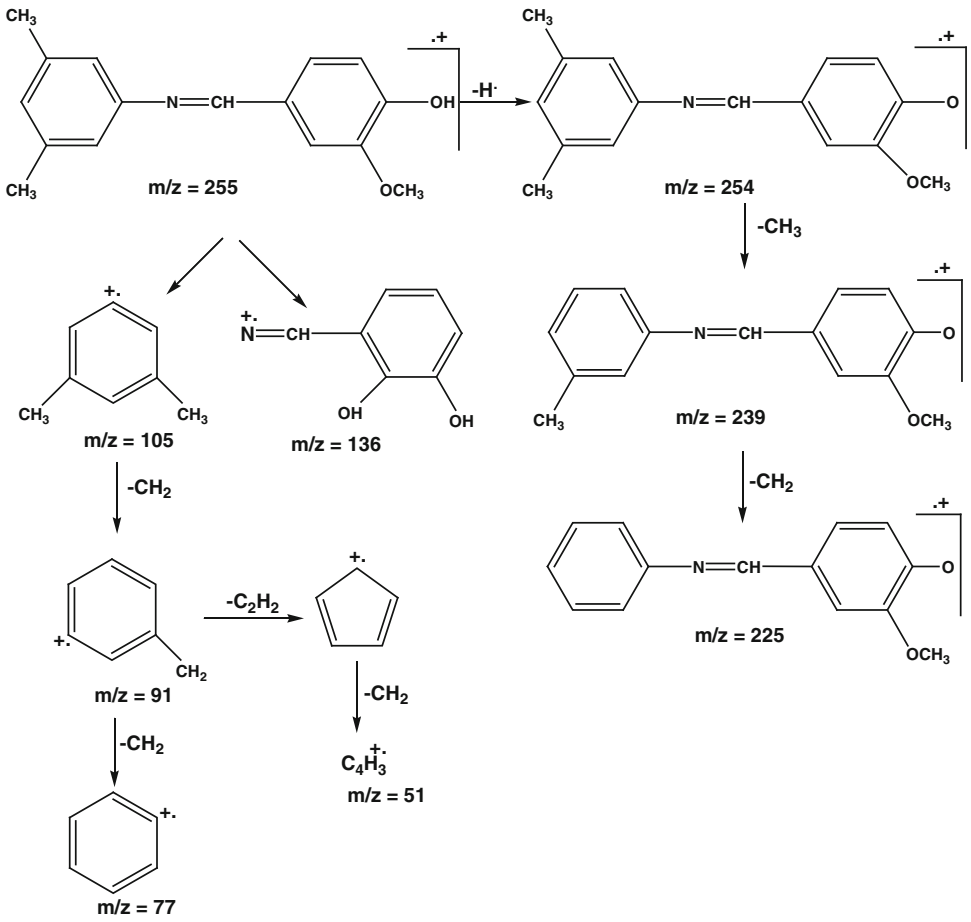

as negative and positive control, respectively. The tubes were incubated at 28 °C for 7 days and growth was determined by measuring linear growth (mm) and growth in the media was determined by measuring linear growth (mm) and growth inhibition was calculated with reference to growth in vehicle control as shown in the following equation:

$$\%\,\text{Growth inhibition} = 100 - \left(\frac{\text{Linear growth in test sample(mm)}}{\text{Linear growth in control(mm)}} \times 100\right) \quad (3)$$

Cytotoxicity

Cytotoxicity was studied by the brineshrimp lethality assay method [41, 42]. Brineshrimp (*Artemia salina*) eggs were hatched in artificial sea water (3.8 g sea salt/L) at room temperature (22–29 °C). After 2 days these shrimps were transferred to vials containing 5 mL of artificial sea water (10 shrimps per vial) with 10, 100 and 1,000 µg/mL final concentrations of each compound taken from their stock solutions of 12 mg/mL in DMSO. After 24 h the number of surviving shrimps was counted. Data were analyzedwith a biostat 2009 computer program (Probit analysis) to determine LD_{50} values.

Results and discussion

Mass spectrometry

The possible suggested molecular ion fragments obtained from the mass spectrum of **HL** measured in positive mode are given in Scheme 4 while its GC-MS spectrum is given in Fig. 1. In Fig. 1 (a) represents the GC spectrum while (b) represents the MS spectrum. In the GC spectrum, a sharp singlet has appeared confirming the purity of the compound. The compound showed a molecular ion peak (parent peak) of maximum intensity with $m/z = 255$. The initial fragmentation is due to the loss of a hydrogen ion giving an ion peak at $m/z = 254$ which is of second maximum intensity. The fragment with $m/z = 254$ gives a mass fragment of $m/z = 239$ by losing CH_3 which then further lose CH_2 group to give a mass fragment of $m/z = 225$.

The molecular ion peak undergoes two major fragmentation pathways with $m/z = 105$ and 136. The former undergoes cleavage to give a mass peak at $m/z = 91$ by the elimination of methylene group (CH_2) and then undergo further fragmentation to give a peak at $m/z = 77$ which can be attributed to the phenyl radical ion. The mass fragment

of $m/z = 91$ undergoes elimination of C_2H_2 group to give a peak at $m/z = 65$ with another rout which then gives an ion peak at m/z = 51 by the elimination of CH_2 group. GS-MS spectrum analysis can not be done for organotin(IV) complexes because of their non-volatile nature.

IR spectra

The IR spectrum of the free ligand was compared with the spectra of tri- and diorganotin(IV) complexes to understand the binding mode of the Schiff base to tin(IV). Weak broad band at 3,320 cm^{-1} in free ligand assigned to (νO–H) was absent in the spectra of all complexes showing the deprotonation of Schiff base which indicates the coordination of Schiff base through phenolic oxygen atom [43]. Further, the IR spectrum of the Schiff base displays a peak at 1,252 cm^{-1}, characteristic of the phenolic (νC-O) vibration, undergoes a positive shift in the spectra of the complexes indicating coordination of the Schiff bases through the phenolic oxygen atom. A strong peak attributable to (νC=N) which occurs at 1,625 cm^{-1} in free ligand as well as in the spectra of all complexes indicating that imine nitrogen atom is not participating in complexation with tin atom. The interesting feature in the spectra of complexes is the appearance of new peaks observed in the region of 546–560 cm^{-1} (νSn-C) and 451–491 cm^{-1} (νSn-O), respectively, confirming the complex formation [44]. This also further supports the coordination of the Schiff bases through the phenolic oxygen atom.

NMR spectra

The conclusion drawn from ^{1}H NMR spectral studies provides further support to the mode of bonding discussed above. A singlet at 6.61 ppm due to the phenolic proton of the Schiff base disappeared in the ^{1}H NMR spectra of the organotin(IV) complexes indicating, thereby, the substitution of the phenolic proton by the organotin(IV) moiety. Other protons in the phenyl rings are found in their normal chemical shift range. The signals at 3.49 ± 0.03 ppm in the Schiff bases assigned to the $-OCH_3$ protons remain unchanged on complexation and thus clearly indicates the non-involvement of this group in complex formation. There is a small upfield shift in the signals of the aromatic protons of the ligand upon complexation with the organotin(IV) moiety. The complexes R_3SnL (**1–5**) and R_2SnClL (**6–8**) show additional signals due to the presence of R groups bonded to Sn(IV). The methyltin (Sn-CH_3) sharp singlet for complex **1** and **6** at 0.64 ppm and 1.08 ppm has $^2J[^{119}Sn\text{-}^1H]$ coupling of 57 and 54 Hz, respectively. In tri- and dibutyltin(IV) complexes the butyl protons appear as multiplets and triplets. The aromatic protons in Ph-Sn appear as multiplet in the range of 6.91–7.77 ppm [45]. In tri-*tert*-butyltin(IV) complex the butyl protons appear as singlet having $^2J[^{119/117}Sn\text{-}^1H]$ coupling of 117, 112 Hz. In tricyclohexynltin(IV) complex the cyclohexyl protons appear as multiplet in the range of 1.30–1.99 ppm [46]. The signal attributable to the imine proton (HC=N) in the spectra of free ligand and all complexes is unaltered and also not flanked by satellites, which indicates non-coordinating behavior of N atom to Sn [47].

In the ^{13}C NMR spectra of the ligand and complexes the peak for imine carbon (C-6) that occurs at 160 ppm remains constant after complexation indicating the non-coordinating behavior of N atom. The ^{13}C NMR spectra of complexes show a slight downfield shift of the phenolic carbon resonances compared with the free ligand. The shift is a consequence of phenolic electron density transfer from the ligand to the acceptor [48]. The downfield shifting of the phenolic carbon in almost all of the complexes indicates the participation of the phenolic group in coordination with tin(IV), i.e., formation of Sn-O bond [49]. The ^{13}C chemical shift of the *ipso*-carbon of the $SnPh_3$ moiety is 139 ppm in $CDCl_3$ solution which indicates the four-coordinated tin specie [50].

The 119Sn NMR spectra of complexes show only a sharp singlet indicating the formation of a single species. However, these values are strongly dependent on the nature and orientation of the organic groups bonded to tin. The shifts observed in complexes can be explained quantitatively in terms of an increase in electron density on the tin atom as the coordination number increases. The ^{119}Sn chemical shift values measured in coordinating solvent for the synthesized compounds show penta-coordination around tin, probably with trigonal bipyrimidal geometry. In non-coordinating solvents, the compounds exist as isolated molecules or ionic-pairs with their tin atoms in pseudo-tetrahedral environments. In coordinating solvents, the tin atoms in the compounds are five-coordinate owing to the participation of the solvent in bonding [51].

Equations 4–7 [52–54] can be used to correlate the coordination pattern of tin(IV) in di- and trimethyltin(IV) derivatives with the $^{1,2}J$ coupling constants: in tetra-coordinated tin compounds ($\theta \leq 112°$) ^1Js are predicted to be smaller than about 400 Hz, whereas ^2Js should be below 60 Hz; for penta-coordinated tin ($\theta = 115–130°$), ^1Js fall in the 450–670 Hz range and the ^2Js fall in the 65–80 Hz range; finally, for hexa-coordinated tin ($\theta = 135°$) ^1Js and ^2Js are generally larger than 670 and 83 Hz, respectively [55]. For methyltin compounds, Eq. 4 (or 5) can be used to give relationship between the magnitude of $|^2J(^{119}Sn,^1H)|$ and the Me-Sn-Me angle θ. A similar behavior in principle is found for $^2J(^{119}Sn,^{13}C)$ but the magnitude of this coupling is less predictable. Equation 8 can be used to relate the bond angle C-Sn-C (θ) for $^nBu_2Sn$ [56, 57]. In the present study the θ values for tri- and dimethyltin(IV) are

110.5° and 109°, respectively, which confirm the tetrahedral geometry around the tin in solution. θ value of 106.9 for $^{2}J(^{119}\mathrm{Sn},^{13}\mathrm{C})$ for tetra-coordinated phenyltin(IV) derivatives has been reported earlier [58], while in present case the value is 107.3 (Table 1).

$$\left|{}^{1}J\left({}^{119}\mathrm{Sn},{}^{13}\mathrm{C}\right)\right| = 11.4\theta - 875 \quad (4)$$

$$\theta = 0.0161\left|{}^{2}J\left({}^{119}\mathrm{Sn},{}^{1}\mathrm{H}\right)\right|^{2} - 1.32\left|{}^{2}J\left({}^{119}\mathrm{Sn},{}^{1}\mathrm{H}\right)\right| + 133.4$$

(In non-coordinating solvents) (5)

$$\theta = 0.0105\left|{}^{2}J\left({}^{119}\mathrm{Sn},{}^{1}\mathrm{H}\right)\right|^{2} - 0.799\left|{}^{2}J\left({}^{119}\mathrm{Sn},{}^{1}\mathrm{H}\right)\right| + 122.4$$

(In coordinating solvents) (6)

$$\left|{}^{1}J\left({}^{119}\mathrm{Sn},{}^{13}\mathrm{C}\right)\right| = (10.7 \pm 0.5)\,\theta - (778 \pm 64) \quad (7)$$

$$\left|{}^{1}J\left({}^{119}\mathrm{Sn},{}^{13}\mathrm{C}\right)\right| = (9.99 \pm 0.73)\,\theta - (746 \pm 100) \quad (8)$$

Table 1 (C-Sn-C) angles (°) based on NMR parameters of selected organotin(IV) derivatives

Compound	$^{1}J(^{119}\mathrm{Sn}$-$^{13}\mathrm{C})$ (Hz)	$^{2}J(^{119}\mathrm{Sn}$-$^{1}\mathrm{H})$ (Hz)	Angle(°)	
			$\theta(1J)$	$\theta(2J)$
1	388.78	57	109.1	110.5
2	395	–	114	–
6	385.5	54	108.7	109
7	398	–	114.5	–

X-ray crystal study

The ortep diagram of 4-((3,5-dimethylphenylimino)methyl)-2-methoxyphenol is shown in Fig. 2 while crystal data, selected bond distances and angles are given in Tables 2 and 3, respectively. Unit cell and H-bonds are shown in Fig. 3. The space group of the crystal is P21. The bond lengths within the phenyl ring range from 1.373(2) to 1.404(3)Å, typical of aromatic character [59]. The structure of the ligand consists of 1D-polymeric chain by H-bonding. The –OH and –OCH_3 are *cis* to each other. The hydroxyl H atom is involved in an intramolecular interaction with the oxygen of the –OCH_3 group. Details of hydrogen bonds are given in Table 4.

UV–visible absorption study of complex-DNA interaction

The interaction of ligand and its and tri- and diorganotin(IV) complexes with DNA were examined by UV–visible spectroscopy, to get some more information about their mode of interaction and binding strength. The effect of varying concentration (0.058–0.23 μM) of DNA on the electronic absorption spectra of 0.392 mM of **HL** and its organotin(IV) complexes were studied and two of representative spectra (compounds 2 and 3) are shown in Figs. 4 and 5. The strong absorption by these compounds in the near UV region (336–352.5 nm) is attributed to the long-living triplet excited state of the aromatic system. The absorption spectra of **HL** upon increasing the concentration of DNA showed gradual decreases in the peak intensities with a small red shift. This phenomenon is usually associated with molecular intercalation into the base stack of

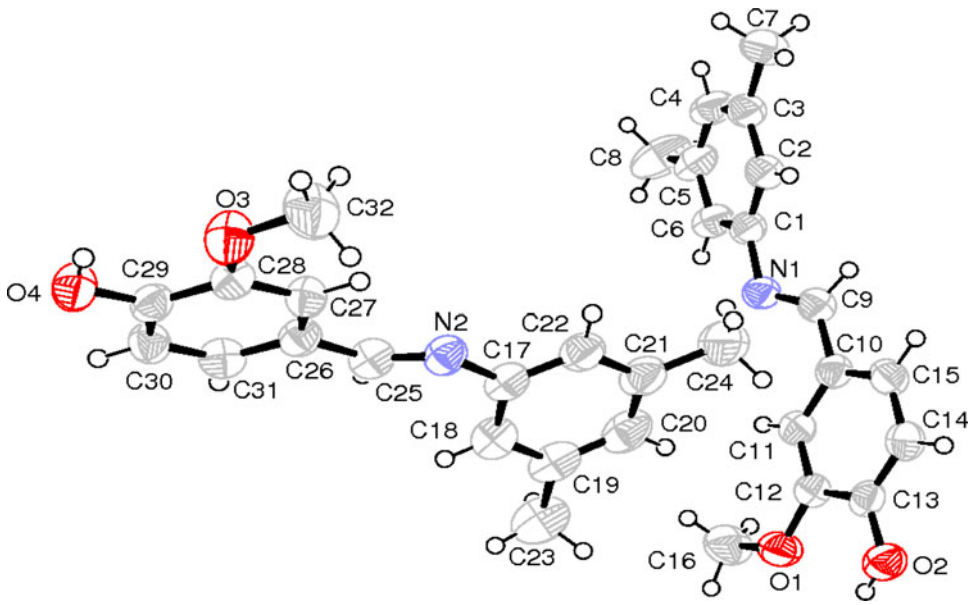

Fig. 2 ORTEP drawing of HL with atomic numbering scheme

Table 2 Crystal data and structure refinement parameters for HL

Formula	C_{16} H_{17} NO_2
Formula weight	255.31
Crystal system	Monoclinic
Space group	P21
a (Å)	8.4750(3)
b (Å)	11.1556(4)
c (Å)	15.1128(6)
α (°)	90
β (°)	90
γ (°)	90
V (Å^3)	1,428.82(9)
Z	4
d (g cm^{-3})	1.187
μ(Mo Kα) (mm^{-1})	0.078
F(000)	544
Crystal habit/size (mm)	Prisms/ 0.40 × 0.30 × 0.25
T (K)	296 (2)
Radiation (Å) (Mo Kα)	0.71073
θ min–max (°)	3.02–25.25
Total reflections	4,151
Tot., Uniq. Data, *R*(int)	5,778, 4,151, 0.0159
Observed data [$I > 0.0$ sigma(I)]	3,566
N_{ref}, N_{par}	4,151, 351
$w = 1/[\sigma^2(\text{Fo})^2 + (0.0468\ P)^2 + 0.0830\ P]$ where $P = [(\text{Fo})^2 + 2(\text{Fc})^2]/3$	
R, wR^2, *S*	0.0336, 0.0802, 1.035
Min. and Max. Resd. Dens. [e/Ang^3]	−0.090, 0.102
Goodness-of-fit	1.035

Table 3 Selected bond lengths (Å) and bond angles (°) for HL

Bond lengths			
O1–C12	1.366(2)	C12–C13	1.404(3)
O1–C16	1.399(3)	C13–C14	1.373(2)
O2–C13	1.355(2)	C1–C6	1.385(3)
N1–C1	1.422(3)	C1–C2	1.387(3)
N1–C9	1.278(3)	C10–C11	1.394(2)
C11–C12	1.376(3)	C3–C7	1.511(4)
Bond angles			
O2–C13–C12	121.95(16)	C11–C12–C13	120.32(16)
O2–C13–C14	118.99(17)	C12–C13–C14	119.06(17)
O1–C12–C13	114.02(17)	C9–C10–C11	122.35(17)
O1–C12–C11	125.66(17)	C2–C1–C6	119.00(19)
N1–C9–C10	124.39(16)	C11–C10–C15	118.75(17)
N1–C1–C6	117.15(17)	C9–C10–C15	118.87(16)
N1–C1–C2	123.75(17)	C10–C11–C12	120.58(17)

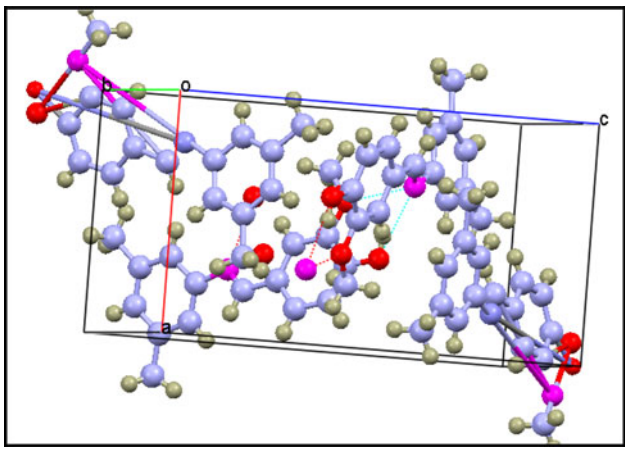

Fig. 3 Unit cell representation of HL viewed along *b*-axis. H-bonding is shown by *dotted lines*

Table 4 Hydrogen-bond geometry (Å, °) for ligand HL

D–H····A	D–H	H····A	D····A	D–H····A
O2–H2····O1	0.8200	2.2500	2.679(2)	113.00
O2–H2····N1	0.8200	2.0700	2.837(2)	156.00
O4–H4····O3	0.8200	2.2300	2.675(2)	114.00
O4–H4····N2	0.8200	2.0700	2.841(2)	156.00
C11–H11····O2	0.9300	2.4900	3.347(2)	154.00
C27–H27····O4	0.9300	2.4900	3.350(2)	154.00

Symmetry codes: (i) $1 - x, -1/2 + y, 1 - z$; (ii) $-x, -1/2 + y, 1 - z$; (iii) $1 + x, y, z$

the DNA [60]. The strength of this electronic interaction is expected to decrease as the cube of the distance between the chromophore and the DNA bases. By decreasing the distance between intercalated **HL** and DNA bases, hypochromism takes place obviously. Thus, this is consistent with the combination of **HL** π electrons and π electrons of DNA bases. Consequently, the energy level of the π–π* electron transition decreases, which causes a red shift. This contributes to the hypochromic effect discussed above [61].

In case of complexes hyperchromism was observed with significant shift in spectral profile which is indication of electrostatic mode of interaction between the negatively charged oxygen of the phosphate group of DNA and the positively charged tin atom, a hard Lewis acid which additionally binds electrostatically to the phosphate backbone of the DNA helix [62]. Hyperchromic effect and hypochromic effect are the spectra features of DNA concerning its double-helix structure.

Based upon the variation in absorbance, the association constants of these complexes with DNA were determined according to Benesi-Hildebrand Eq. 9 [63]:

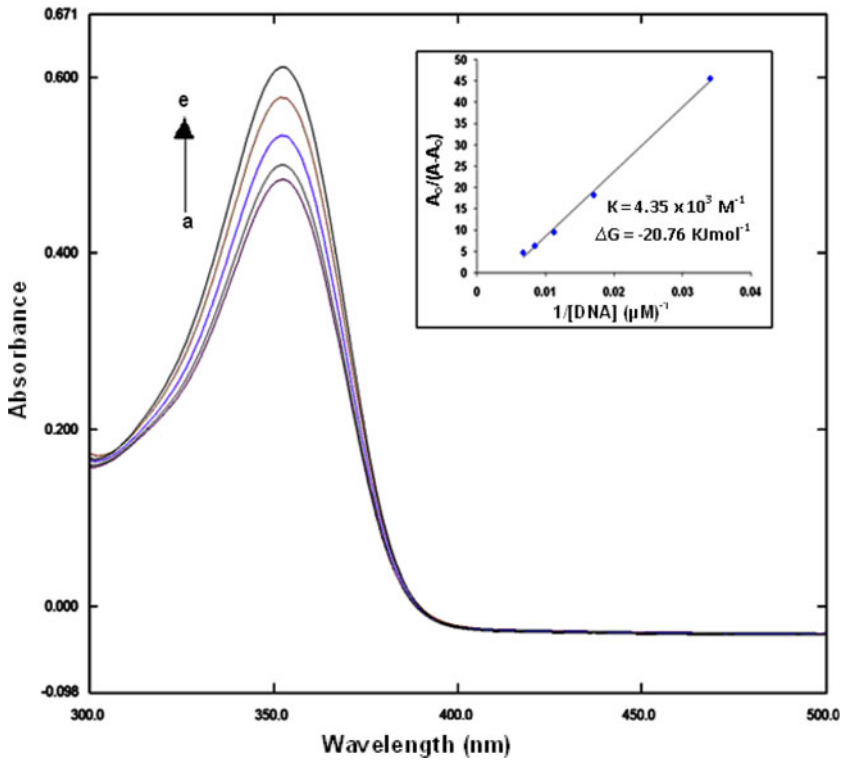

Fig. 4 Absorption spectra of 0.392 mM n-Bu_3SnL in the absence (**a**) and presence of 0.058 μM (**b**), 0.115 μM (**c**), 0.173 μM (**d**), 0.230 μM DNA (**e**). The *arrow direction* indicates increasing concentrations of DNA

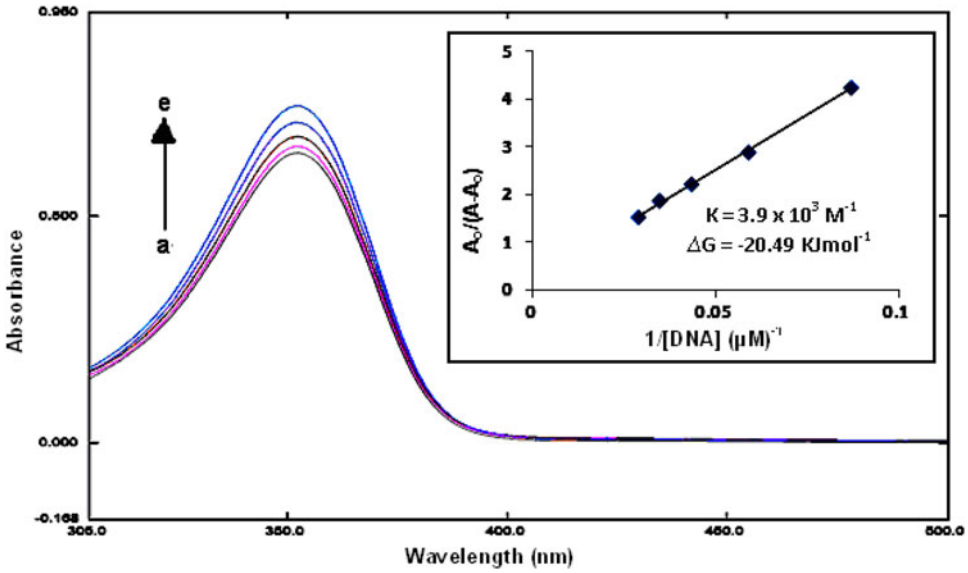

Fig. 5 Absorption spectra of 0.392 mM Ph_3SnL in the absence (**a**) and presence of 0.058 μM (**b**), 0.115 μM (**c**), 0.173 μM (**d**), 0.230 μM DNA (**e**). The *arrow direction* indicates increasing concentrations of DNA

$$\frac{A_0}{A-A_0}=\frac{\varepsilon_G}{\varepsilon_{H-G}-\varepsilon_G}+\frac{\varepsilon_G}{\varepsilon_{H-G}-\varepsilon_G}\frac{1}{K[DNA]} \quad (9)$$

where K is the association constant, A_0 and A are the absorbances of the drug and its complex with DNA, respectively, and ε_G and ε_{H-G} are the absorption coefficients of the drug and the drug-DNA complex, respectively. In order to compare quantitatively the binding strength of the **HL** and its complexes with DNA, the intrinsic binding constants (K or K_b) were obtained by examining the changes in the absorbance for the complexes with increasing concentration of DNA. K_b was obtained from the ratio of slope to the intercept from the plot of 1/[DNA] versus $A_o/A–A_o$. The intrinsic binding constant values (K_b) for the **HL**, **2** and **3** were found to be 1.1×10^4, 4.35×10^3, 3.9×10^3 M^{-1}, respectively. The interaction of these drugs with DNA is a spontaneous process as indicated by their negative values of ΔG (−23.08, −20.76, −20.49 kJ mol^{-1} for **HL**, **2** and **3,** respectively).

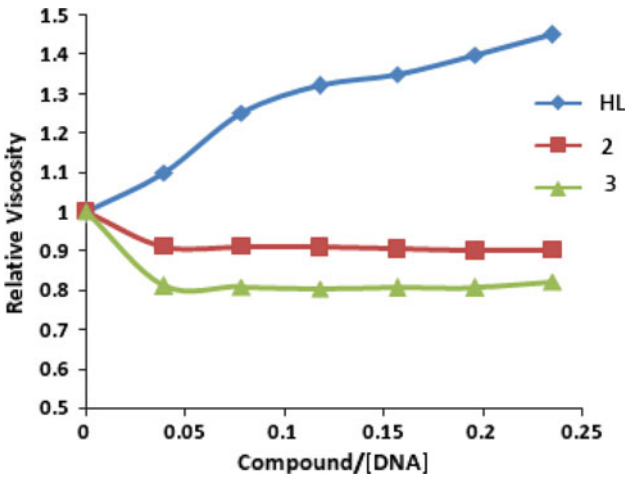

Fig. 6 Effects of increasing amount of HL, compounds **2** and **3** on relative viscosity of CT-DNA at 25 ± 0.1 °C. [DNA] = 2.97 × 10^{-4} M

Viscosity measurement

Binding of small molecules to DNA can change not only the helical twist, but also the contour of length and stiffness (both bending and torsional) and can induce systematic bend into the DNA double helix. A hydrodynamic method such as viscometric measurements in which the solution viscosity of DNA is responsive to the changes in the effective length of DNA molecules is one of the most decisive tests for understanding the binding mode of DNA in solution, i.e., intercalation or other binding modes. Generally, an increase in the relative viscosity is attributed to a length increase of the DNA double helix due to intercalation. On the other hand, a decrease in the relative viscosity due to the reduction of the effective length of DNA molecules results from the bending of the DNA double helix caused by electrostatic interaction between the anion site of phosphate of DNA and the cation site of molecule [64, 65]. The values of relative viscosity $(\eta/\eta_o)^{1/3}$ were calculated from $(t/t_o)^{1/3}$ ratio for all samples, where t, t_o, η and η_o represent the time and viscosity of DNA solution with and without compound, respectively. $(\eta/\eta_o)^{1/3}$ was plotted versus [compound]/[DNA] ratio (Fig. 6). As evidenced from Fig. 6 the relative viscosity of **HL** increases with increasing the [HL]/[DNA] ratio, indicating the intercalative mode of interaction of **HL** with DNA. On the other hand, the relative viscosity of compounds **2** and **3** decreases with increasing the [compound]/[DNA] ratio, indicating the electrostatic mode of interaction of compounds **2** and **3** with DNA. The electrostatic mode of interaction of Sn(IV) complexes is due to the fact that Sn(IV) is a hard acid and prefers to combine with a hard oxygen base. Cationic Sn(IV) exerts electrostatic interaction toward the polyanionic phosphate backbone of DNA due to its hard Lewis acidic property, thus, neutralizing the negative charge of the DNA resulting in significant contraction and conformational changes in the DNA helix that leads to the breakage of the secondary structure of the DNA [66]. The same result has also observed in case of UV–visible spectroscopy as discussed in Sect. 3.4.

Enzymatic study

The effect of various concentrations of **HL** and its organotin(IV) complexes on the activity of the enzyme, Alkaline Phosphatase EC 3.1.3.1 was studied for the hydrolysis of pNPP. Alkaline Phosphatases catalyze the transfer of phosphate groups to water (hydrolysis) or alcohol (transphosphorylation) using a wide variety of phosphomonoesters and are characterized by a high pH optima and a broad substrate specificity [67]. From the study we have observed that the presence of **HL** and its organotin(IV) complexes resulted in the deactivation of the enzyme. The activity of enzyme was markedly decreased by increasing the concentration of **HL** and its organotin(IV) complexes and it was almost completely lost at high concentrations. The remarkable activity of the ligand may be due to OH group, which can play an important role in the enzymatic activity [68]. Among the studied azomethine and its organotin(IV) complexes highest activity was exhibited by Ph_3Sn(IV) derivative. The lower activity of organotin(IV) complexes (except for triphenyltin(IV)) can most probably due to the formation of the stable bond upon complexation between the tin and oxygen atoms. The different behavior of triphenyltin(IV) complex can be due to weaker interactions of ligand with tin because of bulky phenyl groups, thereby regulating the formation of R_3Sn + (IV) moiety that plays a key role in the inhibition of alkaline phosphatase enzyme. The inhibition profile is shown in Fig. 7.

Antioxidant activity

The DPPH radical is a stable free radical (due to extensive delocalization of the unpaired electron) having λ_{max} at 517 nm. When this compound abstracts a hydrogen radical from external source absorption vanishes due to the absence of free electron delocalization [69]. The antioxidant activity of the synthesized ligand **HL** and its organotin(IV) complexes has attracted increasing interests and been noticeably examined. The proposed mechanism for the antioxidant activity of HL and its organotin(IV) complexes is given in Scheme 5. It is evident from Table 5 that the scavenging activity increases with increasing sample concentration in the range tested. As shown in Table 5, the free ligand **HL** has scavenging activity between 9.8 and 74 % within the investigated concentration

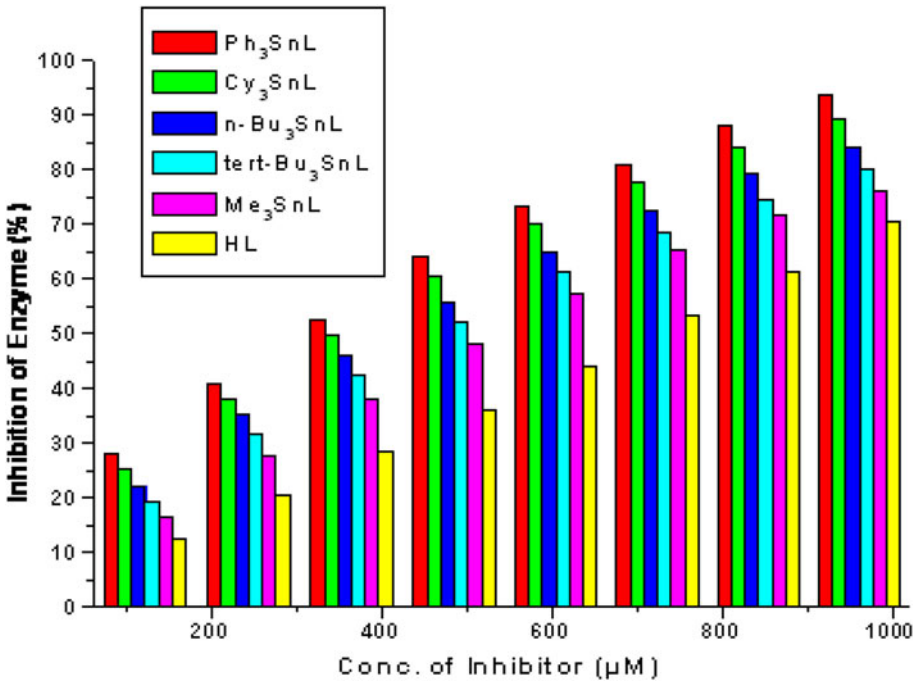

Fig. 7 Inhibition of ALP by HL and its organotin(IV) complexes

Table 5 Antioxidant scavenging activity data of HL and its organotin(IV) complexes on DPPH· free radical at different concentrations

Compounds	DPPH scavenging activity (%) ± SD						
	625 μM	312.5 μM	62.5 μM	31.3 μM	6.3 μM	0.6 μM	0.1 μM
HL	74 ± 0.2	65 ± 0.4	61 ± 0.7	36 ± 0.3	15.1 ± 0.2	12 ± 0.7	9.8 ± 0.8
1	81.3 ± 0.4	58.6 ± 0.9	66 ± 0.3	55.3 ± 1	27.8 ± 0.9	12.2 ± 0.4	9.6 ± 0.2
3	90 ± 0.5	87.3 ± 0.8	56.6 ± 0.7	39.5 ± 0.2	8.9 ± 0.6	7.9 ± 0.9	7.8 ± 0.2
5	80.8 ± 0.2	78.9 ± 0.2	60 ± 0.2	56.6 ± 0.2	27.9 ± 0.2	4.2 ± 0.2	3.8 ± 0.2
7	83.7 ± 0.8	81.7 ± 0.5	80.5 ± 0.2	73.9 ± 0.7	46.96 ± 0.6	13.3 ± 0.7	9.7 ± 0.3
Ascorbic acid	92.3 ± 0.9	92.3 ± 0.5	70.3 ± 1	65.2 ± 0.5	50.3 ± 0.5	30.4 ± 0.4	20.7 ± 0.8

SD standard deviation

range due to the OH group which can react with DPPH radical by the typical H-abstraction reaction (HAT) to form a stable macromolecular radical [70]. The antioxidant activity is increased by the presence of a Sn(IV) metal center, as previously reported for other metals [71]. The maximum activity is shown by phenyltin derivative (compound 3) which has the scavenging activity between 7.8 and 90 %. In free ligand, the abstraction of phenolic hydrogen is easy but in case of complexes the more chances for the hydrogen abstraction is from the CH=N group rather than the OCH_3 group. This is because of the fact that pK_a value of azomethine proton (CH=N) is lower than that of the methoxy proton as it is attached with doubly bounded nitrogen atom. Also azomethine group proton is sp^2 hybridized in nature while that of the methoxy group is sp^3 hybridized. If the hydrogen abstraction comes from CH=N group, the negatively charged comes on the sp^2 carbon and is in conjugation with the benzene ring so the stability of the resulting anion is higher while in case the hydrogen abstraction comes from methoxy group, the negatively charged comes on the sp^2 carbon and is not in conjugation with the benzene ring so the stability of the resulting anion is less.

Antibacterial activity

The synthesized ligand and complexes were screened for antibacterial activity by agar well diffusion [48]. The data are given in Table 6. The data reveal that the ligand shows no activity while its organotin(IV) derivatives show moderate antibacterial activity. However, the antibacterial activity is less than that of the standard drug.

Antifungal activity

The synthesized ligand di- and triorganotin(IV) derivatives of 4-((3,5-dimethylphenylimino)-methyl)-2-methoxyphenol] were tested for their antifungal activity by tube

Scheme 5 Proposed mechanism for the antioxidant activity of **HL** and its organotin(IV) complexes

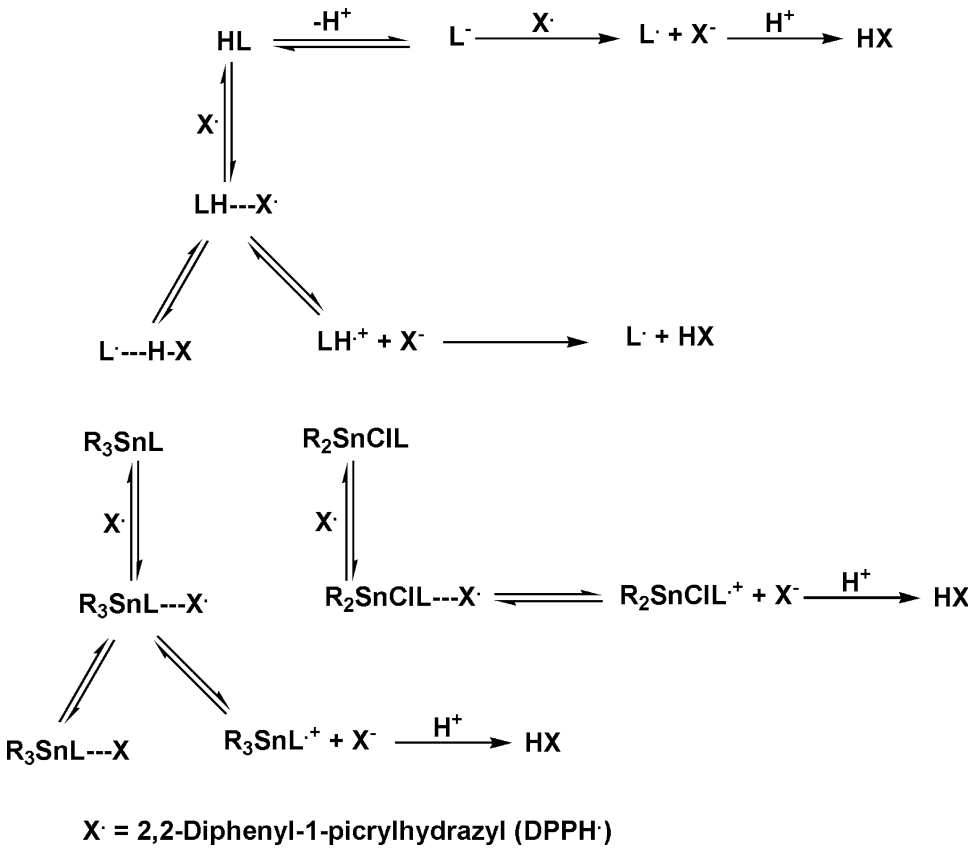

Table 6 Antibacterial activity data of HL and its organotin(IV) compounds

Name of bacterium	Zone of inhibition (mm)							Ref. drugs	
	HL	**(1)**	**(2)**	**(3)**	**(4)**	**(5)**	**(6)**	Roxythromycin	Cefixime
Staphylococcus aureus	–	12	20	20	22.5	14	17	36	22
Klebsiella pneumoniae	–	–	14	18	15	10.5	16	26	21
Micrococcus luteus	–	14	20	15	24	11	13	35	30
Bordetella bronchiseptica	–	14	15	14	19.5	13.5	12	20	16
Escherichia coli	–	16	19	17	–	–	–	26	22
Bordetella bronchiseptica	–	17	19	23	–	–	15	35	26

diffusion [70]. The data are given in Table 7. Most of the compounds showed moderate fungicidal activity as compared with the reference standard drugs. Compound (**3**) is found to be best for the inhibition of fungal growth except in the case of *Candida albicans*, while compound (**2**) has the least activity.

Though the exact biochemical mechanism is not completely understood, the mode of action of antimicrobials may involve various targets in the microorganisms. Metal complexes also disturb the respiration process of the cell and thus block the synthesis of proteins, which restricts further growth of the organisms. This enhancement in inhibiting the growth of bacteria and fungi can also be explained on the basis of their structure. The azomethine linkage and hetero aromatic moiety in the synthesized complexes exhibit extensive biological activities due to increased liposolubility of the molecules in crossing cell membrane of the microorganism. The presence of electron donor group (–OCH_3) in the complexes also plays a role in enhancing the inhibition activity [72, 73].

Cytotoxicity

The cytotoxicity was studied by the brine shrimp lethality method and the results are summarized in Table 8. The LD_{50} data show that all the tested compounds, even the ligand, are toxic with LD_{50} values in the range 0.42–44.55 μg/mL in comparison with reference drug

Table 7 Antifungal[a, b] data of HL and its organotin(IV) compounds

Compound	Percent Inhibition				
	Flavus	*F. solani*	*A. niger*	*Mucor sp.*	*A. fumigates*
HL	35	90	62	30	40
1	65	94	80	80	78
2	20	67	72	43	57
3	24	45	65	54	78
4	25	–	69	35	55
5	32	56	65	45	67
Positive control	100	100	100	100	100

[a] Concentration: 200 μg/mL of media

[b] Percent inhibition of fungal growth $= 100 - g_t/g_c \times 100$, where g_t = linear growth in test (mm) and g_c = linear growth in vehicle control (mm)

Table 8 Cytotoxicity data of HL and its organotin(IV) compounds

Compound	No. of shrimps killed out of 30 per dilution[a]			$LD_{50}^{b,c}$
	1,000 μg/mL	100 μg/mL	10 μg/mL	
HL	29	24	3	44.55
1	30	27	25	0.42
2	30	30	25	5.05
3	30	27	23	1.46
4	30	30	19	8.24
5	30	24	22	1.89
Vehicle control	0	0	0	

[a] Against brine-shrimps (in vitro)

[b] Data is based on mean value of 3 replicates each of 10, 100 and 1,000 μg/mL

[c] Compared with standard drug MS −222 (Tricaine methanesulfonate) with LD50 value of 4.30 μg/mL

MS-222 (*Tricaine Methanesulfonate*) with LD_{50} value 4.3 μg/mL. Complexes **1**, **3** and **5** were the most toxic as compared with tested compounds and reference drugs. The biological activities of the organotin(IV) complexes are comparable to those previously reported [74].

Conductometric study

The conductance of these complexes has been recorded in 80 % ethanol at room temperature in the range 5–19 μS cm^{-1} at 25 °C, suggesting their non-electrolytic nature [75].

Conclusion

The ligand 4-((3,5-dimethylphenylimino)methyl)-2-methoxyphenol was successfully synthesized and characterized by single crystal analysis. The ligand was treated with different di- and triorganotin(IV) chlorides to form the corresponding complexes. The ligand coordinates through oxygen to the Sn atom lead to the formation of four coordinated tin specie. However, the ^{119}Sn-NMR in coordinating solvent (DMSO) gives pseudotetrahedral environments around the tin atom that is due to the coordinating nature of the solvent. The results of UV–visible spectroscopy and viscometry revealed intercalative mode of interaction of **HL** and electrostatic mode of interaction of complexes with DNA. The negative values of Gibb's free energy change show the spontaneity of these interactions. The antimicrobial and cytotoxic activities of triorganotin(IV) derivatives are relatively higher than their corresponding diorganotin(IV) analogues which is due to their greater ability to bind to protein. Moreover, the synthesized compounds show moderate antioxidant activities.

Acknowledgments M. Sirajuddin (Pin# P7-017) gratefully acknowledges the HEC Islamabad, Pakistan, for financial support.

References

1. N. Galic, Z. Cimerman, V. Tomisic, Spectrochim. Acta Part A. **71**, 1274 (2008)
2. W. Rehman, A. Badshah, S. Khan, L.T.A. Tuyet, Europ. J. Medical Chem. **44**, 3981 (2009)
3. R.E. Hester, E.M. Nour, J. Raman Spectrosc. **11**, 49 (1981)
4. E.M. Nour, A.A. Taha, I.S. Alnaimi, Inorg. Chim. Acta. **141**, 139 (1988)
5. E.M. Nour, A.M. Al-Kority, S.A. Sadeek, S.M. Teleb, Synth. React. Inorg. Met. Org. Chem. **23**, 39 (1993)
6. W. Wang, F.L. Zeng, X. Wang, M.Y. Tan, Polyhedron. **15**, 1699 (1996)
7. L. Pellerito, L. Nagy, Coor. Chem. Rev. **224**, 111 (2002)
8. S. Mishra, M. Goyal, A. Singh, Main Group Met. Chem. **25**, 437 (2002)
9. A. Saxena, J.P. Tandon, A.J. Crowe, Polyhedron. **4**, 1085 (1985)
10. A.D. Tiwari, A.K. Mishra, S.B. Mishra, B.B. Mamba, B. Maji, S. Bhattacharya, Spectrochim. Acta Part A. **79**, 1050 (2011)
11. J.S. Casas, A. Castineiras, F. Condori, M.D. Couce, U. Russo, A. Sanchez, R. Seoane, Polyhedron. **22**, 53 (2003)
12. R.G. Zarracino, J.R. Quinones, H. Hopfl, J. Organomet. Chem. **664**, 188 (2002)
13. C. Pettiniari, F. Marchetti, R. Pettiniari, D. Martini, A. Drozdov, S. Troyanov, Synthesis and characterisation of tin(IV) and organotin(IV) derivatives 2-{[(2-hydroxyphenyl) imino]methyl}phenol. Inorg. Chim. Acta. **325**, 103 (2001)
14. S. Tabassum, C. Pettinari, J. Organomet. Chem. **691**, 1761 (2006)
15. M. Gielen, M. Biesemans, R. Willem, Appl. Organomet. Chem. **19**, 440 (2005)
16. P. Yang, M. Guo, Coord. Chem. Rev. **185**, 189 (1999)
17. A.J. Crowe, Antitumor activity of tin compounds, in Metal compounds in cancer therapy, ed. by S. P. Fricker (Chapman & Hall, London, 1994)
18. T.B. Baul, C. Masharing, G. Ruisi, R. Jirasko, M. Holcapek, D. de Vos, D. Wolstenholme, A. Linden, J. Organomet. Chem. **692**, 4849 (2007)
19. H.D. Yin, S.W. Chen, L.W. Li, D.Q. Wang, Inorg. Chim. Acta. **360**, 2215 (2007)

20. H.D. Yin, M. Hong, G. Li, D.Q. Wang, J. Organomet. Chem. **690**, 3714 (2005)
21. M. Cagnoli, A. Alama, F. Barbieri, F. Novelli, C. Bruzzo, F. Sparatore, Anticancer Drugs **9**, 603 (1998)
22. A.G. Davies, P.J. Smith, Adv. Inorg. Chem. Radiochem. **23**, 1 (1980)
23. B.M. Elliot, W.N. Aldridge, J.M. Bridges, J. Biochem. **177**, 461 (1979)
24. S.E.H. Etaiw, A.S. Sultan, A.S.B. El-din, Europ. J. Med. Chem. **46**, 5370 (2011)
25. S.E.H. Etaiw, A.S. Sultan, A.S.B. El-din, M.M. El-bendary, Organomet. Chem. **696**, 1668 (2011)
26. L.S. Lerman, J. Mol. Biol. **3**, 18 (1961)
27. M.J. Waring, *The molecular basis of antibiotic action* (John Wiley and Sons, New York, 1972)
28. R.K. Gilpin, Anal. Chem. **69**, 145R (1997)
29. Y.G. Jun, X.J. Juan, C.H. Yuan, L.Z. Zhou, Chin. J. Chem. **22**, 1325 (2004)
30. M. Rodriguez, A.J. Bard, Anal. Chem. **62**, 2658 (1990)
31. R. Barbieri, L. Pellerito, G. Ruisi, A. Silvestri, A. Barbieri Paulsen, G. Barone, S. Posante, M. Rossi, in *Chemical processes in the marine environment*, eds. by A. Gianguzza, E. Pelizzetti, S. Sammartano (Springer, Berlin, 2000)
32. P.J. Smith (ed.), *Chemistry of Tin* (Blackie Acad. and Prof., London, 1998)
33. W.L.F. Armarego, C.L.L. Chai, *Purification of laboratory chemicals*, 5th edn. (Butterworth-Heinemann, London, 2003)
34. C.V. Sastri, D. Eswaramoorthy, L. Giribabu, B.G. Maiya, J. Inorg. Biochem. **94**, 138 (2003)
35. S. Dey, S. Sarkar, H. Paul, E. Zangrando, P. Chattopadhyay, Polyhedron. **29**, 1583 (2010)
36. J. Ahlers, Biochem. J. **149**, 535 (1975)
37. K. Jiao, W. Sun, H.Y. Wang, Chin. Chem. Lett. **13**, 69 (2002)
38. K. Walter, C. Schütt, in *Methods of enzymatic analysis*, 2nd edn, ed. by H.U. Bergmeyer (Academic Press, New York, 1974)
39. M.M. Hossain, M.F. Aziz, R. Ahmed, M. Hossain, A. Mahmuda, T. Ahmed, M.H. Mazumder, Int. J. Pharm. Sci. **2**, 60 (2010)
40. Z.A. Taha, A.M. Ajlouni, W. Al Momani, A.A. Al-Ghzawi, Spectrochim. Acta Part A. **81**, 570 (2011)
41. A. Rehman, M.I. Choudhary, W.J. Thomsen, *Bioassay techniques for drug development* (Harwood Academic Publishers, Amsterdam, 2001)
42. B.N. Mayer, N.R. Ferrigni, J.E. Putnam, L.B. Jacobson, D.E. Nichols, J.L. Mclaughlin, Planta Med. **45**, 31 (1982)
43. T. Sedaghat, S. Menati, Inorg. Chem. Commun. **7**, 760 (2004)
44. A. Graisa, Y. Farina, E. Yousif, E.E. Saad, Intern. J. Chem. **1**, 34 (2009)
45. S. Shahid, S. Ali, M. Hussain, M. Mazhar, S. Mahmood, S. Rehman, Turk. J. Chem. **26**, 589 (2002)
46. M. Hanif, M. Hussain, S. Ali, M.H. Bhatti, M.S. Ahmed, B. Mirza, H.S. Evans, Turk. J. Chem. **31**, 349 (2007)
47. J.S. Casas, A. Castineiras, F. Condori, M.D. Couce, U. Russo, A. Sanchez, R. Seoane, J. Sordo, J.M. Varela, Polyhedron. **22**, 53 (2003)
48. C. Ma, Y. Han, R. Zhang, Inorg. Chim. Acta. **360**, 2439 (2007)
49. V. Barba, E. Vega, R. Luna, H. Hopfl, I.H. Beltran, S.L. Zamudio-Rivera, J. Organomet. Chem. **692**, 731 (2007)
50. A. Lycka, M. Nadvornik, K. Handlir, J. Holecek, Collect. Czech. Chem. Commun. **49**, 2903 (1984)
51. J. Holecek, A. Lycka, D. Micak, L. Nagy, G. Vanko, J. Brus, S.S.S. Raj, H.K. Fun, S. Weng, Collect. Czech. Chem. Commun. **64**, 1028 (1999)
52. T.P. Lockhart, W.F. Manders, J.J. Zuckerman, J. Am. Chem. Soc. **107**, 4546 (1985)
53. T.P. Lockhart, W.F. Manders, Inorg. Chem. **25**, 892 (1986)
54. T.P. Lockhart, W.F. Manders, J. Am. Chem. Soc. **109**, 7015 (1987)
55. G. Casella, F. Ferrante, G. Saielli, Inorg. Chem. **47**, 4796 (2008)
56. J. Holecek, M. Nadvornik, K. Handlir, A. Lycka, J. Organomet. Chem. **315**, 299 (1986)
57. S.J. Blunden, P.A. Cussack, D.G. Gillies, Magn. Reson. Chem. **24**, 921 (1986)
58. J. Holecek, A. Lycka, K. Handlir, M. Nadvornik, Collect. Czech Chem. Commun. **53**, 571 (1988)
59. F.H. Allen, O. Kennard, D.G. Waston, L. Brammer, A.G. Orpen, R. Taylor, J. Chem. Soc. Perkin Trans. **2**, S1 (1987)
60. A.A. Ensafi, R. Hajian, S. Ebrahimi, J. Braz. Chem. Soc. **20**, 266 (2009)
61. R. Hajian, N. Shams, M. Mohagheghian, J. Braz. Chem. Soc. **20**, 1399 (2009)
62. F.A. Shah, M. Sirajuddin, S. Ali, S.M. Abbas, M.N. Tahir, C. Rizzoli, Inorg. Chim. Acta. **400**, 159 (2013)
63. M. Sirajuddin, S. Ali, A. Badshah, J. Photochem. Photobiol. B **124**, 1 (2013)
64. M. Sirajuddin, S. Ali, N.A. Shah, M.R. Khan, M.N. Tahir, Spectrochim. Acta Part A. **94**, 134 (2012)
65. M. Tariq, N. Muhammad, M. Sirajuddin, S. Ali, N.A. Shah, M.R. Khan, M.N. Tahir, J. Organomet. Chem. **723**, 79 (2013)
66. M.R. Malik, V. Vasylyeva, K. Merz, N. Metzler-Nolte, M. Saleem, S. Ali, A.A. Isab, K.S. Munawar, S. Ahmad, Inorg. Chim. Acta. **376**, 207 (2011)
67. F.J. Huoa, C.X. Yin, Y.B. Wu, P. Yang, Russ. J. Inorg. Chem. **55**, 1087 (2010)
68. C.A. Kontogiorgis, D. Hadjipavlou-Litina, J. Enzyme Inhib, Med. Chem. **18**, 63 (2003)
69. M.C. Foti, C. Daquino, C. Geraci, J. Org. Chem. **69**, 2309 (2004)
70. A. Corona-Bustamante, J.M. Viveros-Paredes, A. Flores-Parra, A.L. Peraza-Campos, F.J. Martinez-Martinez, M.T. Sumaya-Martinez, A. Ramos-Organillo, Molecules **15**, 5445 (2010)
71. S. Ahmad, S. Ali, S. Shahzadi, F. Ahmed, K.M. Khan, Turk. J. Chem. **15**, 5445 (2010)
72. M.A. Neelakantan, M. Esakkiammal, S.S. Mariappan, J. Dharmaraja, T. Jeyakumar, Indian J. Pharm. Sci. **72**, 216 (2010)
73. M.A. Neelakantan, F. Rusalraj, J. Dharmaraja, S. Johnsonraja, T. Jeyakumar, P.M. Sankaranarayana, Spectrochim. Acta A. **71**, 1599 (2008)
74. M. Sirajuddin, S. Ali, A. Haider, N.A. Shah, A. Shah, M.R. Khan, Polyhedron. **40**, 19 (2012)
75. M. Sirajuddin, S. Ali, *Synthesis and characterization of potential bioactive organotins* (LAP Lambert Academic Publishing, Germany, 2013)